Thermal and structural characterization of montmorillonite – poly(vinyl alcohol) nanocomposites

M. TĂMĂŞAN, V. SIMON
„Babeş-Bolyai" University, Faculty of Physics, 1 Kogalniceanu str., 400084 Cluj-Napoca, Romania & Interdisciplinary Research Institute on Bio-Nano-Sciences, 42 Treboniu Laurian str., 400271 Cluj-Napoca, Romania

Clay mineral / polymer nanocomposites have been proposed as very useful materials for a very large range of applications including the field of biomaterials for tissue engineering and systems for drug delivery. Nanocomposites (NCs) synthesized from a montmorillonite clay mineral (MMT) and poly(vinyl alcohol) (PVA) by solution intercalation method with different clay-polymer weight ratios (1:1, 2:1 and 3:1) were characterized from structural, morphologic and thermal points of view. Structural characterization by powder X-ray diffraction analysis allowed evaluating the dispersion of the clay nanoparticles in the polymer matrix by monitoring the position, shape, and intensity of the basal reflections from the silicate layers. The thermogravimetric and differential thermal analysis pointed out the NCs thermal stability and the influence of clay-polymer weight ratios on thermal transitions temperatures. Specific surface and porosimetry analyses by BET method showed a decrease in the specific surface area and in the pore volume of NCs with the decrease of the MMT/PVA ratio. NCs and MMT morphologies were also investigated using transmission electron microscopy.

(Received September 26, 2012; accepted October 20, 2012)

Keywords: Clay-polymer nanocomposites, Montmorillonite, poly(vinyl alcohol), DTA/TGA, XRD, BET, TEM

1. Introduction

Over the last few decades research on the development of new biomaterials for prolonging and improving human health have generated more approaches regarding assembling materials with specific properties that satisfy demands like controlled drug delivery, supporting matrices for tissue recovery, reducing harmful side effects of some drugs and many others [1-3]. In these attempts a new class of nanocomposites based on polymers and on clay minerals was obtained which takes advantage from both these two different materials with new properties suitable for biomedical purposes [4-8].

Starting from tailoring nanoparticles of biodegradable polymers as a controlled drug delivery system it was provided a new way for drugs formulation with a better therapeutic efficacy. Materials with a layered structure that can adapt polar organic compounds between their layers forming a variety of intercalated composites with major potential in the pharmaceutical field have recently begun to be involved in the development of drug delivery and controlled release of active agents systems. Montmorillonite, a bioinert clay mineral with fine grain and large inter-planar spacing in the (001) plane, has superior capability to intercalate large molecules into the interlayer space of the (001) plane. [9-12]. A number of anticancer active drugs were successfully incorporated into polymer-clay composite systems providing promising results in terms of transport and controlled release of the active agents. [9, 10].

Montmorillonite (MMT) is a natural clay mineral belonging to the family of 2:1 phyllosilicates (an alumina octahedral sheet between two tetrahedral silica sheets) with plate–like particles capable of forming stable suspensions in water. This hydrophilic character of MMT promotes the dispersion of the inorganic crystalline layers in water-soluble polymers such as poly(vinyl alcohol) and poly(ethylene oxide) [13]. Polyvinyl alcohol (PVA) is commonly used in medical devices due to specific characteristics such as biocompatibility, high water solubility, good mechanical properties and chemical resistance.

Fundamental studies of the structure, thermal properties and morphology of nanocomposites are important for the understanding of polymer–nanoparticle interactions in order to control structure–property relationships of materials that need to work within the chemical, physical and biological constraints required by any specific application.

The motivation of this study was to obtain and characterize nanocomposites (NCs) from a montmorillonite clay mineral (MMT) and poly(vinyl alcohol) (PVA) by solution intercalation method in different clay-polymer mass ratio (1:1, 2:1 and 3:1) with a higher weight of the clay mineral. The precursors and the composites in powder form were characterized in terms of structural, thermal and textural properties, specific surface area and porosimetry by X-ray diffraction analyses, differential thermal analyses / thermogravimetry, specific surface by BET method and TEM microscopy for the evaluation of the microstructure and phases intercalation. The influence of the clay-polymer mass ratio on the thermal properties of the composites and on their structure and morphology was analyzed and discussed.

2. Experimental

2.1 Materials and preparation method

Materials used as precursors were: a montmorillonite clay mineral purified from a bentonite powder originating in a north-western deposit from Romania and partially crystalline (25%) poly(vinyl alcohol) (here referred as PVA) with 20000 – 30000 molecular weight and 88% degree of hydrolization (supplied by *Acros Organics*).

Purification of the montmorillonite from the bentonite powder was made according to the classical sedimentation method: 100 g of the powder bentonite dispersion in 1 L of double distilled water was mixed at room temperature for 48 h followed by the centrifugation of the solution at 5000 rpm for 20 min. The upper layer of the clay was collected separately and identified by XRD as montmorillonite.

Samples preparation was done by the solution intercalation method. Samples of 1 g, 2 g and 3 g from montmorillonite (for synthesizing three different clay-polymer ratios) were dispersed in 150 ml double distilled water and mixed for 24 h at room temperature to allow the swelling of the clay platelets. The PVA solutions were prepared in three glass beakers by dissolving 1 g of PVA in 150 ml double distilled water in each, heated at 85ºC, mixed on magnetic stirrers at high rotation speed for 24 h. The PVA and MMT solutions were then mixed together at room temperature for 92 h to obtain three composites in 1:1, 2:1 and 3:1 mass ratios. At the final of the mixing stage the solutions were put in the oven at 36ºC to allow the solvent evaporation and composites recovery. The final result was a hardened paste in the case of all three samples which was grounded to powder form using an agate ball mill at a frequency of 30/s for 100 min in order to perform the proposed analyses. The samples were labeled with *MMT –PVA 1:1; MMT –PVA 2:1; MMT-PVA 3:1.*

2.2. Characterization techniques

Differential thermal and thermogravimetric analyses DTA/TGA were performed with Shimadzu DTG-60H equipment from room temperature to 800ºC, in nitrogen and air atmosphere at 70 ml/min flow at 10ºC/min heating speed. The reference material was α-alumina and alumina open crucibles were used as samples and reference support. X-ray diffraction analyses were made on a Shimadzu XRD -6000 diffractometer using Ni-filtered CuKα radiation (wavelength λ = 1.5418 Å) operating in Bragg – Brentano θ – 2θ geometry at a scanning speed of 2º/min. All measurements were taken using a generator voltage of 40 kV and a current of 30 mA. Specific surface area and pore volume were determined by nitrogen adsorption experiments on a BET Surface Area Analyzer, QSURF M3. The equipment is designed for specific surface areas ranging from 0.10 to 2000 m^2/g, with an accuracy of 0.01 m^2/g; automatic calibration, maximum degassing temperature 300°C. TEM analyses were carried out on a Jeol JEM 1010 microscope.

3. Results and discussions

3.1 DTA/TG characterizations

The DTA and TG recordings for precursors and MMT-PVA composites (Fig. 1) revealed their thermal behaviour up to 800ºC as well as the influence of the clay-polymer ratio on melting and decomposition temperatures in the PVA phase. The first endothermic peak observed in all DTA curves in the temperature range 40-180ºC with the maximum at70ºC is assigned to the evaporation of physically adsorbed water from the samples surface. The maximum temperature of the endothermic peak representing the melting process in PVA (which for the semicrystalline polymers is considered to be the melting temperature) is 196ºC while in the composites this temperature is shifted towards smaller values in small steps with the MMT content increasing. On the other hand, the onset temperature of the melting peak is shifted to higher values as the MMT content is increased; for the MMT–PVA 3:1 sample the melting peak is indistinguishable. These details can be seen in Fig. 2 where an insight at the melting region are presented for PVA and composites.

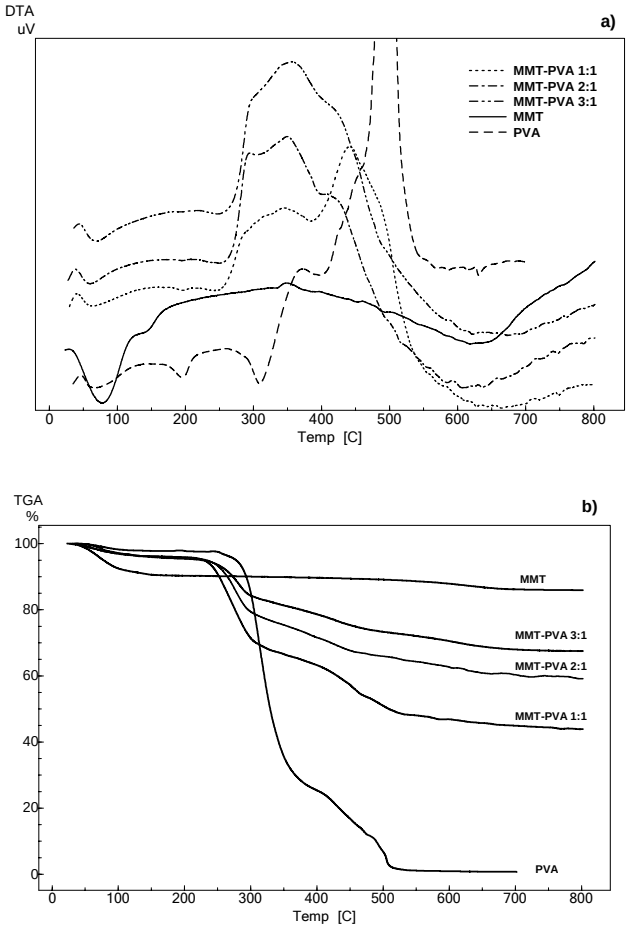

Fig. 1. Thermal analyses of composites and precursors: DTA signals (a) and TG signals (b).

The values of the onset, endset and peak temperatures as well as the corresponding mass losses for all thermal events identified in DTA curves are summarized in Table 1. The shift of the polymer melting temperature in composites to lower values is accompanied by the decreasing of the peaks intensity and consequently the decreasing of the melting heat. This effect may occur due to a decreased mobility of the polymer chains caused by the intercalation of some polymer chains between the clay interlayers and therefore the decreasing of the crystallinity in the PVA phase.

The thermal decomposition of PVA was reported in a previous paper of the authors regarding another type of nanocomposite [14]. Briefly this decomposition followed a multistep process with the overlapping of some decomposition steps and a total mass loss of 96.7%. It starts with an endothermic peak in 250-400ºC range and maximum at 310ºC with a corresponding mass loss of 73%. This process can be associated with the decomposition of the polymer by chain-scission reactions and the elimination of the volatile products, mainly water [15]. The second and third decomposition steps identified in the TG curve with corresponding mass losses of 13% and 11% may be attributed to elimination reactions of side-chains or side-groups and consequently cyclization reactions with char formation. The composites thermograms denote a different behaviour starting with the decomposition onset temperature, above 245ºC, where the ΔT signal is rising, giving a first exothermic peak at 315ºC, followed by a second exothermic peak at 345ºC. The last exothermic peak is at 440ºC in the MMT-PVA 1:1 sample. Similar behaviour presented the other two samples with differences in the onset and peak temperatures shifted toward lower values along with MMT content. Comparing the composites thermograms with that of the PVA's it can be seen that unlike in the polymer the first decomposition stage is related to an *exothermic* event that may be linked to the release of the hydrogen bonds between the polymer and clay sheets as a consequence of a higher energy configuration. The second decomposition stage in the composites is also related to an exothermic event of higher energy level which could be the result of the overlapping of clay dehidroxylation process with the second decomposition stage in the polymeric phase. And finally, the third exothermic peak, indicated by a shoulder following the previous peak can be related to the final decomposition stage of the organic phase accompanied by the releasing of the volatile byproducts. Analyzing the thermograms (Fig. 1 b) a good thermal stability of the composite with a smaller content of clay (MMT-PVA 1:1) is revealed comparable with that of the polymer, having both the onset temperature of the first decomposition peak at 245ºC. According to the clay content the total mass loss is reduced in the samples with higher clay ratio. The thermal behavior of MMT is given by two mass losses identified in its DTA/TG curves: the free water removal region in the temperature below 200°C with 10% mass loss and the structural water region in the temperature range 500-800°C with a mass loss of 3-4%.

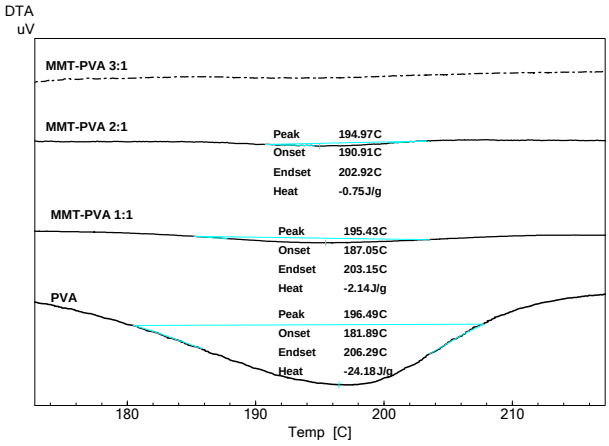

Fig. 2. DTA in the PVA melting region for PVA and composites.

Table 1. Thermal event temperatures and corresponding mass loss

Sample	Peak I			Peak II PVA melting		Peak III I[st] degradation step			Peak IV II[nd] and III[rd] degradation steps			Total mass loss (%)
	$T_o - T_e$ (ºC)	T_{max} (ºC)	Mass loss I (%)	$T_o - T_e$ (ºC)	T_{max} (ºC)	$T_o - T_e$ (ºC)	T_{max} (ºC)	Mass loss III (%)	$T_o - T_e$ (ºC)	T_{max} (ºC)	Mass loss IV (%)	
MMT	31 – 120	68	10	–	–	–	–	–	400 – 800	660	3	13
PVA	45 – 135	67	2	182 – 206	196	245 – 400	310	72.3	400 – 475	ΔT ↗	13.4	98.7
									475 – 550	500	11	
MMT-PVA 1:1	41 - 160	71	4	183 - 208	195	245 - 330	315	27	330 - 385	345	3.6	50.6
									385 - 490	440	16	
MMT-PVA 2:1	40 - 160	61	3.9	184 - 206	194	208 - 312	295	17.8	312 - 403	349	6.8	39.2
									403 - 664	ΔT↘	10.7	
MMT-PVA 3:1	44 - 184	69	4.4	–	–	210 - 302	ΔT ↗	11.1	302 - 420	355	6.8	28.6
									420 - 584	ΔT↘	6.3	

3.2 XRD characterizations

The clay and composites diffractograms are presented in Fig. 3. The crystalline phases identified in the clay mineral are montmorillonite $Na_{0.3}(Al, Mg)_2Si_4O_{10}(OH)_2 \cdot 4H_2O$ (diffraction file JCPDS 29-1498) and a second phase of SiO_2 (cristobalite, diffraction file JCPDS 139-1425). The same peaks are present in the composites diffractograms with few differences in the first diffraction peak that corresponds to the (001) reflections on the silicate clay layers.

The intercalation of the polymer between the clay interlayers can be well characterized from powder X-ray diffraction by calculating the increase of the basal d-spacing and shifting of the diffraction angle to lower values. [16] The peak at $2\theta = 6.7^{\circ}$ from the pristine MMT diffractogram correspond to the (001) reflections on the clay planes giving an interplanar distance of 13.18 Å. The d_{001} peaks of MMT-PVA samples appeared at lower angles than in MMT case and higher interlayer spacings are calculated from Bragg's law with the increase of the polymer content; this may indicate that a part of the polymer chains are intercalated into the silicate interlayers following the expanding of the basal spacings. The values of the interlayers spacing, diffraction angles and interlayers expansions are summarized in Table 2. An additional small peak found at 2θ around 9º with a corresponding d-spacing of 9.2-9.6 Å may be a result of some no intercalated layers. [17]. Moreover, all diffractograms of nanocomposites exhibit a higher background than one would expect for simple mixtures of PVA and MMT, implying the existence of some exfoliated inorganic layers throughout the polymer matrix, conclusions that are sustained by TEM images and porosimetry evaluation by BET method. These results lead to the conclusion that the clay-polymer composites developed an intercalated hybrid structure containing also a small part of exfoliated clay layers.

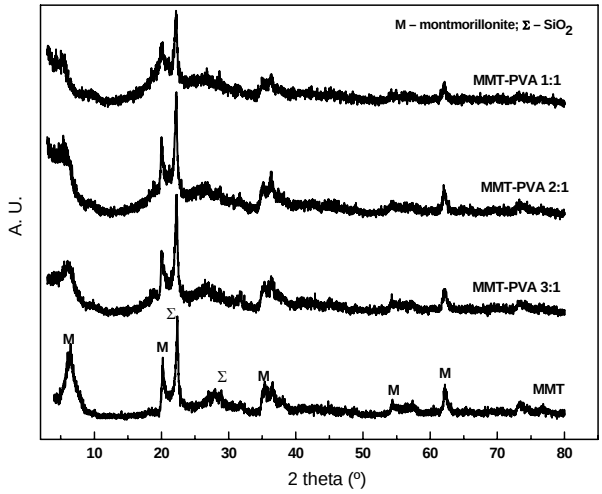

Fig. 3. XRD patterns of MMT and MMT-PVA composites.

Table 2. First diffraction angles and interlayer spacing for MMT and MMT-PVA composite.

Sample	2θ (degrees)	Basal *d*-spacing (Å)	*d*-spacing increasing (Å)
MMT/PVA 1:1	5.37	16.42	3.24
MMT/PVA 2:1	5.44	16.23	3.05
MMT/PVA 3:1	5.98	14.77	1.59
MMT	6.70	13.18	

3.3 TEM investigations

Additional to the global averaging results given by XRD the Transmission Electron Microscopy can directly provide information in real space, in a specific area, concerning the morphology and crystalline or amorphous structures as well as the homogeneity of the samples.

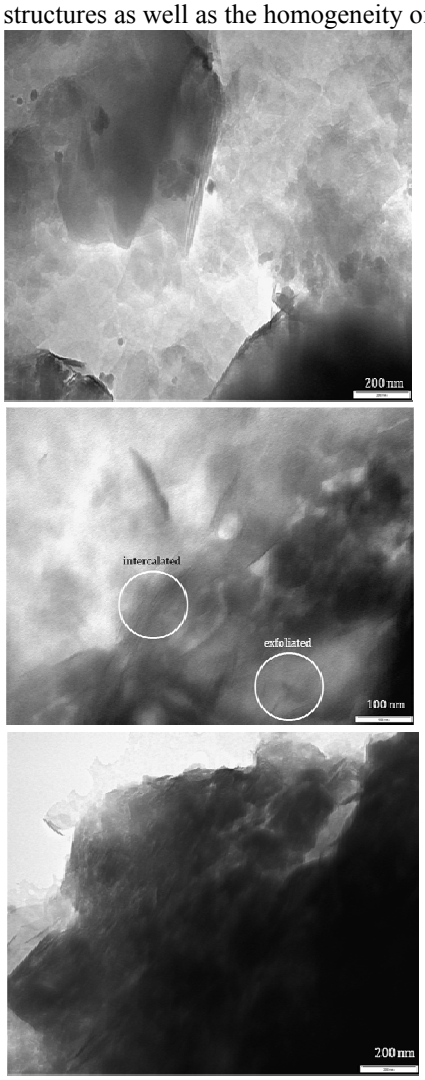

(a) MMT

(b) MMT-PVA 1-1

(c) MMT-PVA 2-1

Fig. 4. TEM images of clay and nanocomposites.

The silicate layers of the clay are composed of heavier elements (Al, Si, O) than the interlayer and surrounding polymeric matrix (C, H, N) therefore in TEM images they appear darker in bright field images.

TEM images of MMT and of nanocomposites MMT-PVA 1:1 and MMT-PVA 2:1 (Fig. 4) obtained on the samples in powder form reveal the distribution and dispersion of the nanoparticles within the polymer matrix. Well ordered stacking of clay platelets are observed in TEM image of MMT (Fig. 4a) while the images of nanocomposites (Fig. 4 b,c) show the coexistence of stacked clay layers with few separate exfoliated layers. Line bars are indicated on the figures.

3.4 Specific surface area and porosimetry determinations

Specific surface area and porosimetry analyses were determined by measuring isotherm adsorption/desorption of nitrogen at 77K (Brunauer–Emmett–Teller method) on the basis of BET equation. The measurements were taken in 1 point (one gas mixture) and 3 points (three gas mixtures) while the porosimetry was determined by 13 gas mixtures. The values resulted from the analyses for these parameters are presented in Table 3. The specific surface area of MMT lays around 58 m^2/g while the composites present smaller values with increasing of the polymer content probably as a consequence of filling or obturating of the pores by the polymer chains.

The distribution of pore volumes and pore sizes in the MMT and MMT-PVA 3-1, illustrated in Fig. 5 and Fig. 6, respectively, denote both micro- and meso-pores, with a larger extent of the mesopores. In the nanocomposite sample a similar evolution of the pore volume distribution is followed but at smaller values.

Table 3. Specific surface area and total pore volume of MMT and nanocomposites.

Sample	1 point BET surface area m^2g^{-1}	3 points BET surface area $/m^2g^{-1}$	Total pore volume $/cm^3g^{-1}$
MMT	58.7196	57.7631	0.1182
MMT/PVA 3:1	8.6874	10.1669	0.0373
MMT-PVA 2:1	2.2298	3.0589	0.0183
MMT-PVA 1:1	0.233	–	–

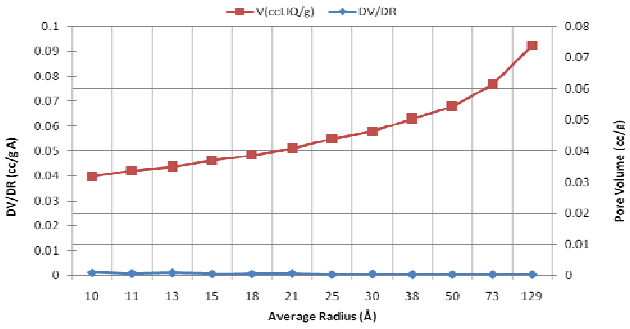

Fig. 5. Pore size and pore volume distribution by BET method for MMT clay.

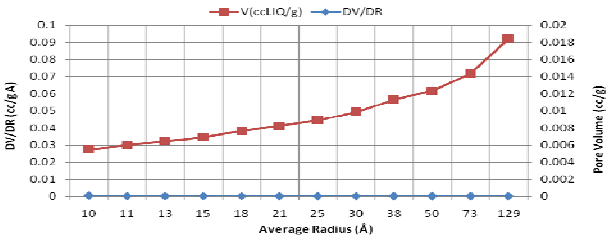

Fig. 6. Pore size and pore volume distribution by BET method for MMT-PVA 3-1 nanocomposite.

4. Conclusions

Montmorillonite – poly(vinyl alcohol) nanocomposites were prepared in three clay-polymer mass ratios (1:1, 2:1, 3:1) by solution intercalation method. The intercalation of the organic – inorganic phases in the composites was assessed by structural, thermal and morphologic analyses performed on the precursors and hybrid materials. Differential thermal analyses combined with thermogravimetry highlighted the distinct thermal behavior of composites with respect to the precursors and indicated the development of chemical bonding between the organic and inorganic phase, and the influence of the clay-polymer ratio on the temperature of thermal events. The onset temperature of the first decomposition stage indicated a higher thermal stability for the MMT-PVA 1:1 sample.

Based on XRD data, the expansion of the clay interlayers calculated for MMT-PVA 1:1 and MMT-PVA 2:1 samples was up to 3 Å, while for MMT-PVA 3:1 sample the gallery expansion attained only 1.5 Å. XRD, TEM and BET results point out that these MMT-PVA composites are organised at nanoscale in a hybrid structure where both intercalated and exfoliated silicate layers coexist. According to thermal and structural properties of the investigated nanocomposites, in view of biomedical applications, the sample with lower clay content is recommended for further investigations.

Acknowledgements

This work was possible with the financial support of the Sectoral Operational Programme for Human Resources Development 2007-2013, co-financed by the European Social Fund, under the project number POSDRU 89/1.5/S/60189 with the title **„Postdoctoral Programs for Sustainable Development in a Knowledge Based Society”**, and the PNII Idei PCCE-248/2008 project granted by the Romanian National University Research Council – CNCSIS Romania.

References

[1] G. Carja, G. Lehutu, L. Dartu, M. Mertens, P. Cool, Appl. Clay Sci. **65-66**, 37 (2012).
[2] R. Zamiri, Z. Azmi, M. Bin Ahmad, K. Shameli, M. Darroudi, M.A. Mahdi, M.S. Husin, J. Optoelectron. Adv. Mater. **12**, 1879 (2010).
[3] G. Carja, H. Niiyama, G. Ciobanu, T. Aida, Mater. Sci. Eng. C **27**, 1129 (2007).
[4] N. Salahuddin, E.-R. Kenawy, R. Abdeen, J. Appl. Polym. Sci. **125**, E157 (2012).
[5] L.C. Bandeira, P.S. Calefi, K.J. Ciuffi, E.H. de Faria, E.J. Nassar, M.A. Vicente, R. Trujillano, R. Polym. Int. **6** , 1170 (2012).
[6] I. Grecu, G. Strat, S. Gurlui, V. Grecu, I. Lihtetchi, M. Strat, S. Stratulat, C. Picealca, J. Optoelectron. Adv. Mater. **10**, 1408 (2008).
[7] M. Miculescu, G. Motiu, M. Radut, D. Donescu, M.C. Corobea, J. Optoelectron. Adv. Mater. **9**, 3364 (2007).
[8] E.M. Seftel, E. Dvininov, D. Lutic, E. Popovici, C. Ciocoiu, J. Optoelectron. Adv. Mater. **7**, 2869 (2005).
[9] S.S. Feng, M. Lin, A. Panneerselvan, C.W. Gan, W. Zhou, Biomaterials **30**, 3297 (2009).
[10] B. Sun, B. Ranganathana, S.-S. Feng, Biomaterials **29**, 475 (2008).
[11] Y.H. Lee, T.F. Kuo, B.Y. Chen, Y.K. Feng, Y.R. Wen, W.C. Lin, F.H. Lin, Biomed. Eng.- App. Bas. Commun. **17**, 72 (2005).
[12] Y.C. Dong, S.S. Feng, Biomaterials **26**, 6068 (2005).
[13] K.E. Strawhecker, E. Manias, Chem. Mater. **12**, 2943 (2000).
[14] M. Tamasan, V. Simon, Dig. J. Nanomater. Bios. **6**, 1311 (2011).
[15] B.J. Holland, J.N. Hay, Polymer **42**, 6775 (2001).
[16] E. Ruiz-Hitzky, A. Van Meerbeek, Clay mineral– and organoclay–polymer nanocomposites. In: F. Bergaya, B.K.G. Theng, G. Lagaly (Eds.), Handbook of Clay Science. Elsevier, Amsterdam, 2006, pp. 583-621.
[17] S.I. Yun, D. Attard, V. Lo, J. Davis, H. Li, B. Latella, F. Tsvetkov, H. Noorman, S. Moricca, R. Knott, H. Hanley, M. Morcom, G.P. Simon, G.E. Gadd, J. Appl. Polym. Sci. **108**, 1550 (2008).

*Corresponding author: viorica.simon@phys.ubbcluj.ro